PCCP

Accepted Manuscript

ROYAL SOCIETY OF CHEMISTRY

www.rsc.org/pccp

drogen are metastable: no measurable ortho-para conversion in solid pure $H_2@C_{60}$ has been observed in experiments that lasted several days at cryogenic temperatures.[12,20–23] In both the para- and ortho-$H_2@C_{60}$ manifold, the energy difference between the ground states and the lowest excited states is in the order of 22 meV, equivalent to 255 K.[21,23,24] Given the typical energy level separations and the ortho-para metastability, only the respective rotational ground states, ortho-H_2 with $J = 1, I = 1$ and para-H_2 with $J = 0, I = 0$, are effectively populated at any temperature below 50 K. In the following discussion we neglect the nuclear spin degrees of freedom and the nuclear spin structure of the rotational energy levels, except for Pauli exclusion principle effects.

The ortho-H_2 ground rotational state consists of three rotational sub-levels with angular momentum $J = 1$. In the gas phase these rotational sub-levels have the same energy. If the icosahedral symmetry of C_{60} is maintained, the three-fold degeneracy should be preserved for hydrogen confined inside the fullerene cage. However the degeneracy of the rotational sub-levels could be lifted in the presence of local perturbations with lower than cubic symmetry. Kohama et al. reported an anomaly in the temperature dependence of the specific heat of $H_2@C_{60}$ and interpreted the observation assuming a lifted degeneracy for the $J = 1$ ground state of ortho-hydrogen but were unable to identify exactly the type and nature of the symmetry breaking mechanism on a microscopic level.[31] In particular it was not possible to establish to which extent inter-cage interactions are responsible for lowering the symmetry depending on the packing of the molecules in the solid.

In the solid phase the centres of the C_{60} molecules are arranged according to a cubic packing. Solid C_{60} crosses several phase transitions on cooling reflecting variations in the dynamics and structural order of the rotational degrees of freedom.[32] At room temperature the C_{60} molecules rotate almost isotropically[33] and the crystal symmetry is face centred cubic (fcc)[34]. Below 255 K, free reorientation is replaced by a ratcheting motion among symmetry equivalent configurations[33] and the low temperature crystal structure of C_{60} is simple cubic ($Pa\bar{3}$) with 4 inequivalent oriented molecules located at one edge and on the centres of the xy, xz and yz faces of the unit cubic cell.[34] In the low temperature phase, the orientation of the C_{60} molecules in the unit cell depends on the detail of the intermolecular potential. The inter-cage interaction potential has two minima with an energy difference of 11.4 meV separated by barrier of 290 meV.[32] These two minima correspond to two possible orientations of neighbouring molecules: in the lowest energy configuration the double bond of one molecule lays opposite to a pentagonal face of a neighbouring molecule (P-orientation) while in the slightly higher energy minimum the double bond of one molecule lays opposite to a hexagonal face (H-orientation), respectively.[35,36] Below 90 K large amplitude molecular re-orientation is inhibited and the proportion of molecules in the two orientations freezes out.[34] At ambient pressure about 85% of the molecules exist in the P-orientation below 90 K while the remainder are in the H-orientation.[37] However if pressure is applied at high temperature and maintained while cooling, the fraction of molecules in the P-orientation is reduced: for example at a pressure of 5 kbar the P-oriented fraction reduces to less than 15%.[37] Interestingly for our study, the site symmetry at the centre of the C_{60} cages is axial ($\bar{3}$) in both orientations with the symmetry axis pointing along principal diagonals of the cubic unit cell.[32]

Here we employ inelastic neutron scattering (INS) to elucidate the effects of symmetry breaking interactions in the quantum dynamics of $H_2@C_{60}$. INS is able to provide distinctive insight into the energy level structure of H_2 confined in fullerene cages.[23–25,38] Indeed INS has the unique capability to access ortho-para transitions in which the total molecular nuclear spin is flipped simultaneously with a change in the rotational state. In this new investigation, the temperature dependence of the INS line corresponding to the transition between the ortho-to-para $J = 1$ to $J = 0$ states is studied in order to determine the structure of the ortho-$H_2@C_{60}$ ground state. By using pressure to change the inter-cage potential in a prescribed manner, we can investigate the origin of the symmetry breaking leading to the lifting of the $J = 1$ rotational degeneracy. The comparative changes in the INS line in experiments with and without pressure provide direct evidence that the lifted degeneracy in $H_2@C_{60}$ is related to inter-cage interactions in the solid phase.

2 Experimental details

$H_2@C_{60}$ was synthesized by the "molecular surgery" procedure devised by Komatsu and co-workers.[2] In this way all of the fullerene cages are occupied by a guest H_2 molecule. The sample used in the experiments was synthesized by the group lead by Turro from Columbia University (NY).[24,25] In the final stage of the preparation the sample was sublimed to remove occluded solvents and residual impurities. The purified powdered sample with mass 107 mg was thinly wrapped in an aluminium foil sachet for the neutron scattering experiments. Neutron powder diffraction confirmed that the sample was in the cubic phase characteristic of highly pure C_{60} fullerene.

The INS experiments were conducted on the IN5b time-of-flight (TOF) spectrometer at the Institut Laue-Langevin (ILL) in Grenoble, France.[39] All the spectra were recorded at 8 Å for the incident neutron wavelength. In the chosen set-up the instrumental resolution, described by a Gaussian profile, was 0.3 meV (full width at half maximum) in the neutron energy gain region around -14.5 meV, where the $H_2@C_{60}$ transition of interest is located. The temperature dependence of the INS line corresponding to the transitions from the ground ortho-H_2 state to the para-H_2 ground state (neutron energy gain) was studied first without and then with an applied pressure of 5 kbar. For the experiments conducted at ambient pressure, the sample was mounted inside a ^{3}He/^{4}He dilution refrigerator inserted into a standard ILL 'orange cryostat'. Stable sample temperatures in the range $60\,\text{mK} \leq T \leq 35\,\text{K}$ were achieved. In the experiments with applied pressure, the sample was subjected to hydrostatic pressure up to 5 kbar using ^{4}He as the medium. The pressure cell was mounted directly inside the 'orange cryostat' providing a base temperature of 3.3 K for the pressure experiments. The data recorded in this investigation is openly available.[40]

3 Results

3.1 Experiments at ambient pressure

The temperature dependence of the inelastic line corresponding to transitions from the ground ortho-H_2 state to the para-H_2 ground state (neutron energy gain) is shown in figure 1. In total 20 datasets were recorded between 35 K and 60 mK at approximately equal steps in the logarithm of temperature, but for clarity only a selection is shown in the figure. Although no structure is fully resolved, the line gets broader and asymmetric, with its centre shifting towards the left (higher neutron energy gain) when the temperature is increased.

The change in line-shape, line-width and peak position, with temperature is inconsistent with transitions from a three-fold degenerate level. A multi-component analysis of the temperature dependence of the line was attempted by assuming an axially-symmetric perturbation, so that the $J = 1$ ortho ground state is split into one non-degenerate level and one doubly-degenerate level. Panel a) of figure 2 shows the best fit of the experimental line-shapes to a two-component Gaussian model:

$$N(E;T) = \frac{1}{1+2\exp[-\Delta/k_BT]}\frac{\overline{N}}{\sqrt{2\pi}\sigma}\exp\left[-\frac{(E-\overline{E})^2}{2\sigma^2}\right] + \\ + \frac{2\exp[-\Delta/k_BT]}{1+2\exp[-\Delta/k_BT]}\frac{\overline{N}}{\sqrt{2\pi}\sigma}\exp\left[-\frac{(E-\overline{E}+\Delta)^2}{2\sigma^2}\right] \quad (1)$$

where $\overline{E}$ is (minus) the energy of the non degenerate energy level with respect to the para ground state, Δ is the energy separation between the non-degenerate and the doubly degenerate ortho-levels, $\overline{N}$ is the total number of counts and σ is related to the full width at half maximum of each component $w = 2\sqrt{2\log(2)}\sigma$. In this model the relative intensity of the two components is constrained only by Δ and by the degeneracy of the levels. The experimental data sets were fitted simultaneously for all the recorded temperatures by using $\overline{E}$, Δ, $\overline{N}$ and w as fitting parameters. A linear correction of the background was performed at each temperature before fitting the lines in order to reduce the effects of small systematic errors. The fits reveal a crossover in the relative intensities of the two components with increasing temperature. The observations can only be explained with a model in which the low-energy state is non-degenerate and the high-energy state is two-fold degenerate. The best fit values are $\overline{N} = 19.8 \pm 0.2$ for the transition counts, $\overline{E} = -14.60 \pm 0.01$ meV for the centre of the low-energy line, $\Delta = 0.135 \pm 0.01$ meV for the energy separation between the low-energy non-degenerate state and the double degenerate state and $w = 0.45 \pm 0.01$ meV for the full width at half maximum. The corresponding structure of the rotational ground states of $H_2@C_{60}$ is shown in panel b) of figure 2.

The total number of scattered neutrons integrated over the experimental line remains constant with temperature within error bars. The constancy of the counts $\overline{N}$ indicates that: a) any spin conversion effect is negligible in the time scale of the experiment (3 days), b) at all the temperatures of interest for this study (less than 40 K) no other ortho state is appreciably populated but the ground state and c) there is no dependence of the transition probabilities on the ortho initial state, as discussed below.

3.2 Experiments in the pressure cell

To gain insight into the influence of inter-cage interactions, hydrostatic pressure was applied to the sample. The application of pressure affects the sample in two ways: (a) it changes the lattice constant and consequently the distance between cages, which influences the inter-cage interaction potential and (b) it modifies the statistical weights of the P-oriented and H-oriented fullerenes.

In the first set of pressure experiments hydrostatic pressure at 5 kbar was applied to the sample starting from 140 K. The sample was kept under pressure at 5 kbar and cooled down to be studied between 20 K and 3 K. The analysis of the neutron powder diffraction data, recorded simultaneously with the INS spectra, implied a volumetric compression of the unit cell of the order of 5%. In such experimental conditions the fraction of H-oriented versus the P-oriented molecules was increased to about 85%[37] allowing a study of the ortho-para INS line in the H-rich phase at 5 kbar. In a second set of experiments the temperature was raised to 50 K, the pressure was released, the sample was cooled down and the line was studied again between 20 K and 3 K. In this last set of experiments, contrary to the experiments conducted entirely at ambient pressure, most of the fullerenes are expected to remain locked into the H-orientation with minimal influence on the unit cell parameters.

The low temperature INS spectra of $H_2@C_{60}$ kept under pressure at 5 kbar (applied from 140 K) and after releasing the pressure are shown in panel a) and b) of figure 3, respectively. Since all the materials that encase the sample (aluminium foil, pressure cell, cryostat) are in the ground state at the temperatures of the study, no peaks other than the $J = 1$ to $J = 0$ transition of $H_2@C_{60}$ are visible in this region of neutron energy gain and 'empty cell' subtraction was not needed in the data analysis.

The best fit of each set of lines with the two component model of equation 1 is shown in figure 3.

3.3 Discussion

The best fit values for the two-Gaussian model parameters are reported in table 1 for each of the three set of experiments. Although the variation in the position of the centre of the lower energy component $\overline{E}$ is not significant because of experimental uncertainties, a clear trend in the splitting of the ortho-$H_2@C_{60}$ ground state can be observed across the three different sets of experiments. The splitting Δ gets larger going from the P-rich phase to the H-rich phase and again to the H-rich phase with applied pressure: the maximum variation in Δ is about 40% between the P-rich phase and the H-rich phase under pressure. These observations indicate that the relative orientation and the distance between cages play a significant role in lifting the degeneracy of the ortho-$H_2@C_{60}$ ground state. This is also seen by plotting the temperature dependence of the first moments of the best-fit model to the rotational INS peak, see figure 4. The range of variation and the turning point of the curves describing the temperature dependence of the first moments are determined by Δ, since Δ influences both the Boltzmann factor determining the relative weight of the two components as well as their absolute splitting. Although it is not possible to establish the asymptotic low-temperature trend

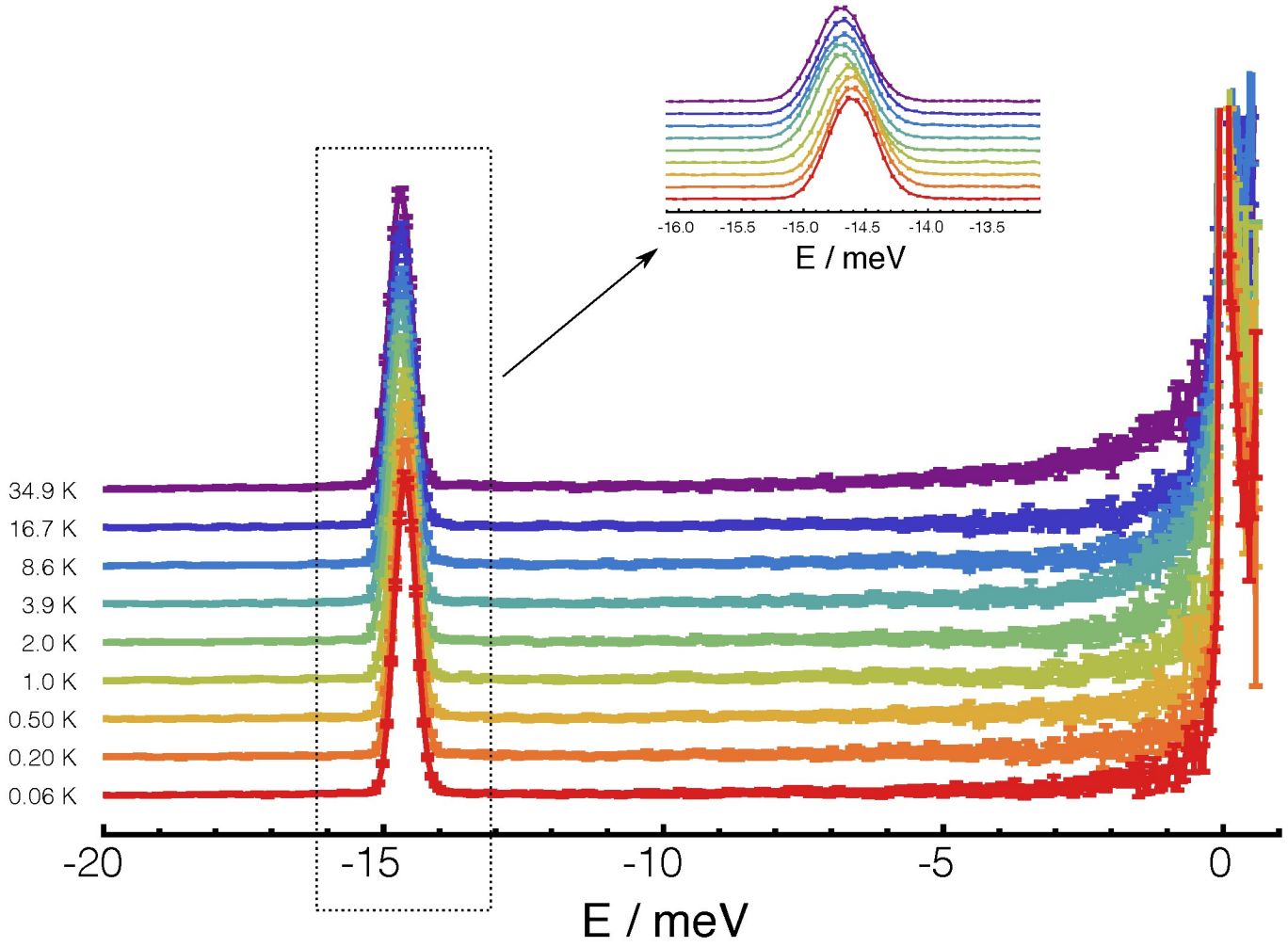

Fig. 1 Low temperature INS spectra of $H_2@C_{60}$ at 8 Å in neutron energy gain. The dashed box encloses the region containing the peak from the ortho to the para ground state and is zoomed in the inset for clarity.

for the datasets recorded in the pressure cell, the slope of the curves and the temperature at which the curves begin to rise with decreasing temperature, confirm the larger splitting in the H-rich phase as determined by the detailed line-shape fits, either with or without pressure, than in the P-rich phase at no applied pressure.

In all the three sets of experiments the full widths at half maximum are slightly larger than the instrumental resolution allowing us to estimate the inherent line-width of the ortho to para transitions between 0.3 and 0.4 meV.

Table 1 Summary of the best fit values of the energy parameters entering in the two Gaussian model of equation 1 for the three experimental datasets.

	P-rich phase Ambient pressure	H-rich phase Ambient pressure	H-rich phase 5 kbar
$\bar{E}$/meV	-14.60 ± 0.01	-14.58 ± 0.02	-14.56 ± 0.01
Δ/meV	0.135 ± 0.01	0.17 ± 0.02	0.19 ± 0.02
w/meV	0.45 ± 0.01	0.46 ± 0.02	0.46 ± 0.01

4 Quantum dynamics and INS transition probabilities

A good basis for the study of the five-dimensional quantum dynamics of a "rigid" H_2 confined inside a C_{60} cage is given by the product of a translational wave-function $\psi_{NLM}(\mathbf{R})$ with a rotational wave-function $Y_{JM_J}(\theta_\mathbf{r}, \phi_\mathbf{r})$, where $\mathbf{R} = \{R, \theta_\mathbf{R}, \phi_\mathbf{R}\}$ and $\mathbf{r} = \{r, \theta_\mathbf{r}, \phi_\mathbf{r}\}$ are the spherical coordinates of centre of mass and the internuclear vector of the H_2 molecule, respectively.[20,21,27] The rotational wave-functions are spherical harmonics Y_{JM_J} identified by the rotational angular momentum J and its projection along a fixed quantisation axis M_J.[41] The translational wave-functions can be decomposed into the product of of a radial wave-function $\psi_{NL}(R)$ with a spherical harmonic $Y_{LM_L}(\theta_\mathbf{R}, \phi_\mathbf{R})$ where N is the principal (energy) quantum number and L and M_L are the orbital angular momentum quantum numbers. Within a very good approximation the ground state ortho wave-functions are a linear combination of $\psi^o_{00}(R)Y_{00}(\theta_\mathbf{R}, \phi_\mathbf{R})Y_{1m}(\theta_\mathbf{r}, \phi_\mathbf{r})$ with $m = -1, 0, 1$. The ground para state wave-function is $\psi^p_{00}(R)Y_{00}(\theta_\mathbf{R}, \phi_\mathbf{R})Y_{00}(\theta_\mathbf{r}, \phi_\mathbf{r})$.[3,4,20,21] At the lowest order in perturbation theory only the rank 2 harmonics of

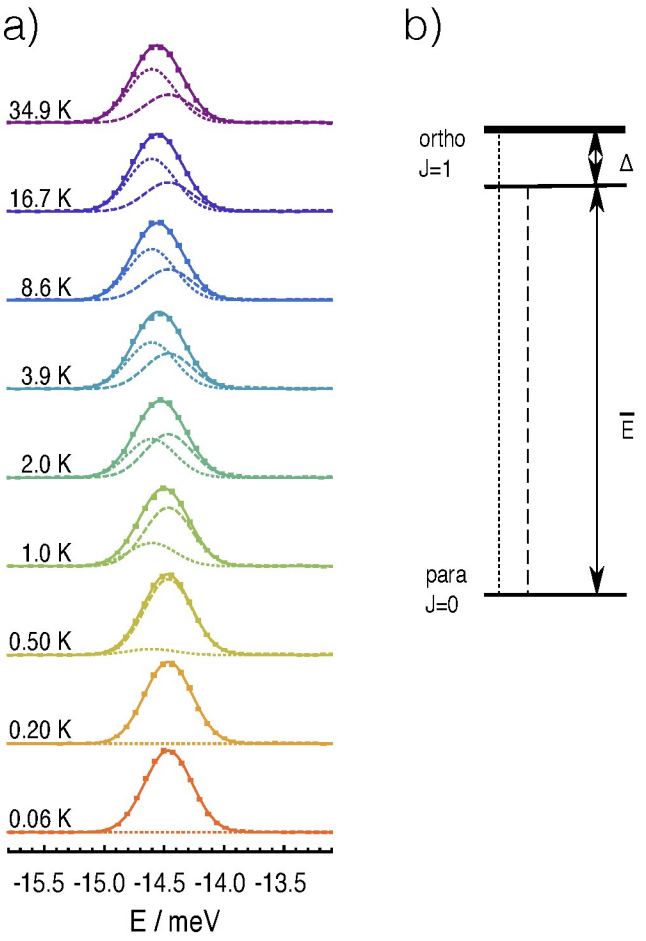

Fig. 2 a) Experimental INS spectra of the ground state transitions of $H_2@C_{60}$ at various temperatures with error bars (points) and best fit with the two Gaussian model of equation 1 (lines). The best fit curve is shown as full line for each temperature, while the two components are shown as dashed and dotted lines, respectively. For clarity only data at few selected temperatures are shown. b) The structure of the two lowest rotational state of $H_2@C_{60}$ as determined from the analysis of the INS experiments.

the crystal field potential make a contribution to the quantum dynamics of $J=1$ ortho ground state.[42] Any symmetry breaking potential with the principal axis pointing along the Z laboratory frame is effectively equivalent to:

$$V=\sqrt{20\pi}\delta\left\{Y_{20}(\theta_{\mathbf{r}},\phi_{\mathbf{r}})+\frac{\eta}{\sqrt{6}}\left[Y_{22}(\theta_{\mathbf{r}},\phi_{\mathbf{r}})+Y_{2-2}(\theta_{\mathbf{r}},\phi_{\mathbf{r}})\right]\right\} \quad (2)$$

where δ and η represent the anisotropy and the bi-axiality of the potential respectively. In the ortho state the solutions of the restricted quantum dynamical problem are

$$\Psi_{1n}=\sum_{m=-1}^{1}\psi_0^o(R)Y_{00}(\theta_{\mathbf{R}},\phi_{\mathbf{R}})Y_{1m}(\theta_{\mathbf{r}},\phi_{\mathbf{r}})c_{mn} \quad n=-1,0,1, \quad (3)$$

where c_{mn} are coefficients of a unitary matrix. The energies are $E_{10}=2\delta$ and $E_{1\pm1}=-\delta(1\pm\eta)$.

For a crystal field whose principal axis frame orientation is defined by the Euler angles Ω_{CF}, the eigenstates are obtained by rotation

$$\Psi'_{1n}=\sum_{m,m'=-1}^{1}\psi_0^o(R)Y_{00}(\theta_{\mathbf{R}},\phi_{\mathbf{R}})Y_{1m'}(\theta_{\mathbf{r}},\phi_{\mathbf{r}})D^1_{m'm}(\Omega_{CF})c_{mn} \quad (4)$$

where $D^1_{mn}(\Omega_{CF})$ are the coefficients of the rank 1 Wigner matrix[41] rotating the states from the laboratory frame to the crystal field frame. The para ground state is a scalar $\Psi'_{00}=\Psi_{00}$. Clearly the energy of the levels does not depend on the orientation of the crystal field with respect to the laboratory frame.

As far as intensities are concerned, the number of scattered neutrons is given by

$$N_{tot}(T)=c\sum_n p_{1n}(T)\overline{W}_{00\leftarrow 1n} \quad (5)$$

where c is a constant depending on the experimental details, $p_{1n}(T)$ is the temperature dependent Boltzmann population of the level $1n$ and $\overline{W}_{00\leftarrow 1n}$ represents the transition probability for a transition between the $1n$ ortho-$H_2@C_{60}$ sub-level and the (non-degenerate) 00 para-$H_2@C_{60}$ ground state. Elaborating the treatment of Yildirim et al.[43] the transition probability for the ortho to para transitions can be written as

$$\begin{aligned}W_{00\leftarrow 1n}&=\frac{k_f}{k_i}\frac{b^2}{4}\left|\left\langle\Psi'_{00}\left|e^{i\mathbf{q}\cdot\mathbf{R}}\sin\left(\frac{\mathbf{q}\cdot\mathbf{r}}{2}\right)\right|\Psi'_{1n}\right\rangle\right|^2\\&=\frac{k_f}{k_i}\frac{b^2}{4}\left[\left\langle\psi^p_{00}(R)\left|j_0(qR)\right|\psi^o_{00}(R)\right\rangle j_1\left(\frac{qr}{2}\right)\right]^2\times\\&\times 4\pi\left|\sum_{m,m'}Y_{1m'}(\theta_{\mathbf{q}},\phi_{\mathbf{q}})D^1_{m'm}(\Omega_{CF})c_{mn}\right|^2\end{aligned} \quad (6)$$

which depends on the crystallite orientation via $D^1_{mn}(\Omega_{CF})$. Here k_i and k_f are the modulus of the incident and scattered neutron wave-vector, $\mathbf{q}=\mathbf{k}_f-\mathbf{k}_i$ is the transferred wave-vector, b is the incoherent scattering length of bound ^{1}H and j_0 and j_1 are the order 0 and 1 spherical Bessel functions of first kind[44]. However for an isotropic powder the transition probability simplifies to:

$$\overline{W}_{00\leftarrow 1n}=\frac{k_f}{k_i}\frac{b^2}{4}\left[\left\langle\psi^p_{00}(R)\left|j_0(qR)\right|\psi^o_{00}(R)\right\rangle j_1\left(\frac{qr}{2}\right)\right]^2 \quad (7)$$

after averaging over the crystallites orientations.

The experimental observations are consistent with an axial crystal field ($\eta=0$) so that there is one singly degenerate level with energy $E_{10}=-2\delta$ and a double degenerate level with energy $E_{1\pm1}=\delta$. This is in agreement with the expected low temperatures crystal structure of C_{60} as discussed in the introduction. From the experimental splittings, $\delta=-0.045\pm0.003$ meV for $H_2@C_{60}$ molecules in the P-rich phase at ambient pressure and δ increases a further 25% and 40% in absolute value in the H-rich phase at no applied pressure and at 5 kbar, respectively. Equation 7 proves that the transition probability is independent of the state $1n$, justifying the assumptions on which the line-shape analysis is based.

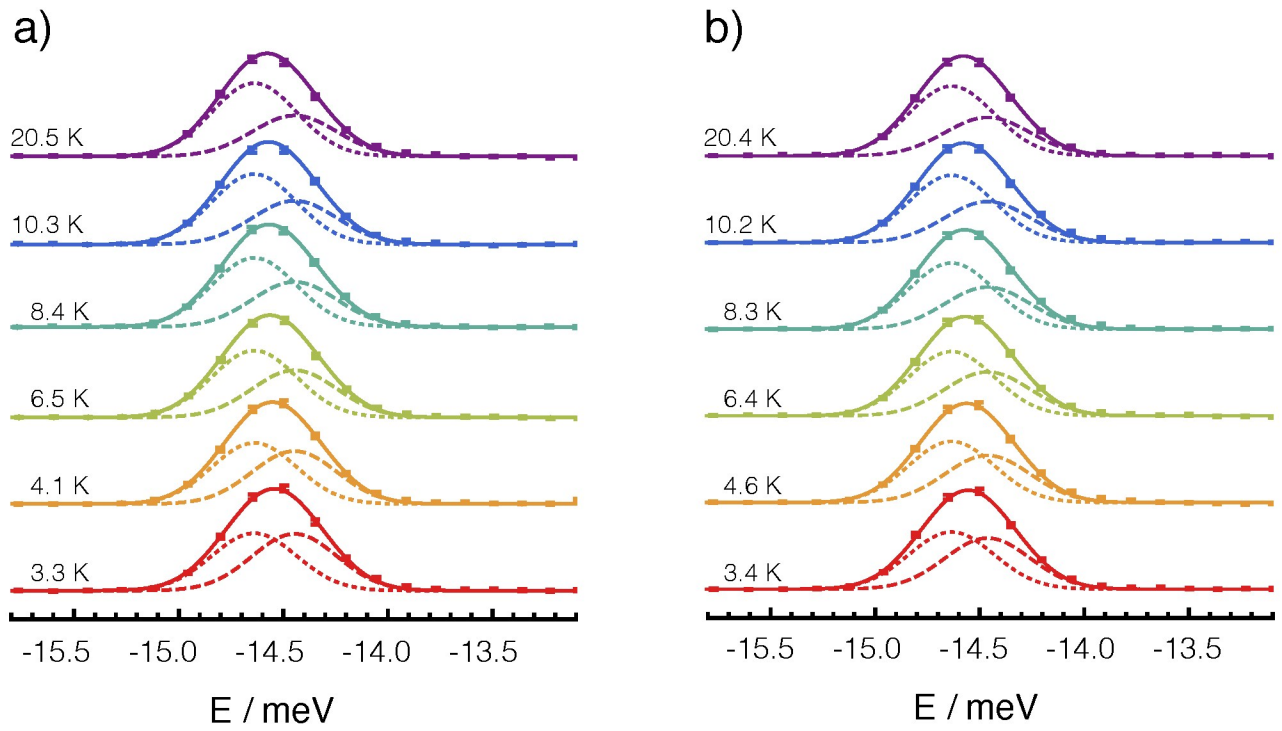

Fig. 3 Inelastic neutron scattering spectra of $H_2@C_{60}$ in energy gain around -14.6 meV in the H-rich phase a) at 5 kbar applied pressure and b) at ambient pressure after releasing the pressure at 50 K. Experimental data are represented by points with error bars. The best fit curve with a two Gaussian model is shown as full line for each temperature, while the two components are shown as dashed and dotted lines, respectively. The peak corresponds to INS transitions from the $J = 1$ ortho states to $J = 0$ para state (neutron energy gain).

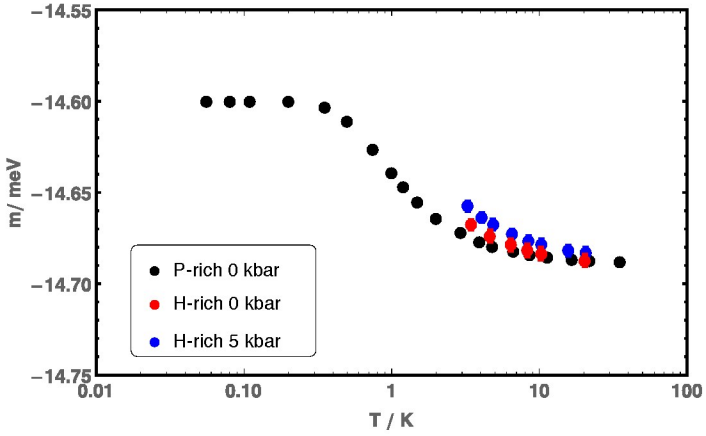

Fig. 4 The temperature dependence of first moments of the best-fit model, equation 1, to the INS line for the dataset in the P-rich phase at ambient pressure (black dots), H-rich phase at ambient pressure (red dots) and H-rich phase at 5 kbar (blue dots).

5 Conclusions

The fine structure of the ortho-$H_2@C_{60}$ ground state has been studied by probing the INS transition between the $J = 1$ and $J = 0$ state in energy gain on the IN5b TOF spectrometer at the ILL, Grenoble. The experimental observations demonstrated that the three-fold degeneracy of the rotational ortho-H_2 ground state is lifted in $H_2@C_{60}$ in the solid phase. It was possible to determine that the three sub-levels with $J = 1$, composing the ground state of ortho-$H_2@C_{60}$, are split into a lower non-degenerate level and a higher double degenerate level shifted 0.135 meV above. The effect of pressure on the fine structure of the $J = 1$ to $J = 0$ line has been investigated as well. Application of pressure affects the size of the splitting of the ortho ground state of $H_2@C_{60}$ by modifying the lattice parameter and the orientation of neighbouring molecules. It was observed that the experimental splitting increased by 40% following the application of pressures up to 5 kbar. Although our findings cannot exclude contributions from the reduction in the icosahedral symmetry of the fullerenes, possibly related to the presence of the enclosed hydrogen itself, they conclusively show that the symmetry breaking effects in $H_2@C_{60}$ are influenced to a large extent by the orientation and proximity of the neighbouring molecules.

6 Acknowledgements

This work was funded by the UK Engineering and Physical Sciences Research Council (EPSRC) under grant number EP/M001970/1. The authors are indebted to Nicholas J. Turro for providing the original samples and Mark Denning for purifying it. The authors thank Claude Payre and James Maurice from ILL for their help in setting up the high pressure cell.

References

1 M. H. Levitt, *Philosophical Transactions of the Royal Society A: Mathematical, Physical and Engineering Sciences*, 2013, **371**, 20120429.

2 K. Komatsu, M. Murata and Y. Murata, *Science*, 2005, **307**, 238–240.

3 M. Xu, F. Sebastianelli, Z. Bačić, R. Lawler and N. J. Turro, *The Journal of Chemical Physics*, 2008, **128**, 011101.

4 M. Xu, F. Sebastianelli, Z. Bačić, R. Lawler and N. J. Turro, *The Journal of Chemical Physics*, 2008, **129**, 064313.

5 M. Xu, F. Sebastianelli, B. R. Gibbons, Z. Bačić, R. Lawler and N. J. Turro, *Journal of Chemical Physics*, 2009, **130**, 1–14.

6 M. Xu and Z. Bačić, *Physical Review B*, 2011, **84**, 195445.

7 M. Xu, L. Ulivi, M. Celli, D. Colognesi and Z. Bačić, *Physical Review B*, 2011, **83**, 241403.

8 M. Xu, S. Ye, A. Powers, R. Lawler, N. J. Turro and Z. Bačić, *The Journal of Chemical Physics*, 2013, **139**, 064309.

9 M. Xu, S. Ye and Z. Bačić, *The Journal of Physical Chemistry Letters*, 2015, **6**, 3721–3725.

10 B. Poirier, *The Journal of Chemical Physics*, 2015, **143**, 101104.

11 E. Sartori, M. Ruzzi, N. J. Turro, J. D. Decatur, D. C. Doetschman, R. G. Lawler, A. L. Buchachenko, Y. Murata and K. Komatsu, *Journal of the American Chemical Society*, 2006, **128**, 14752–14753.

12 M. Carravetta, A. Danquigny, S. Mamone, F. Cuda, O. G. Johannessen, I. Heinmaa, K. Panesar, R. Stern, M. C. Grossel, A. J. Horsewill, A. Samoson, M. Murata, Y. Murata, K. Komatsu and M. H. Levitt, *Physical Chemistry Chemical Physics*, 2007, **9**, 4879–4894.

13 E. Sartori, M. Ruzzi, R. G. Lawler and N. J. Turro, *Journal of the American Chemical Society*, 2008, **130**, 12752–12756.

14 N. J. Turro, A. A. Martí, J. Y.-C. Chen, S. Jockusch, R. G. Lawler, M. Ruzzi, E. Sartori, S.-C. Chuang, K. Komatsu and Y. Murata, *Journal of the American Chemical Society*, 2008, **130**, 10506–10507.

15 J. Y.-C. Chen, A. A. Martí, N. J. Turro, K. Komatsu, Y. Murata and R. G. Lawler, *The Journal of Physical Chemistry B*, 2010, **114**, 14689–14695.

16 N. J. Turro, J. Y.-C. Chen, E. Sartori, M. Ruzzi, A. A. Martí, R. G. Lawler, S. Jockusch, J. López-Gejo, K. Komatsu and Y. Murata, *Accounts of Chemical Research*, 2010, **43**, 335–345.

17 Y. Li, X. Lei, R. G. Lawler, Y. Murata, K. Komatsu and N. J. Turro, *The Journal of Physical Chemistry Letters*, 2010, **1**, 2135–2138.

18 A. Zoleo, R. G. Lawler, X. Lei, Y. Li, Y. Murata, K. Komatsu, M. Di Valentin, M. Ruzzi and N. J. Turro, *Journal of the American Chemical Society*, 2012, **134**, 12881–12884.

19 V. Filidou, S. Mamone, S. Simmons, S. D. Karlen, H. L. Anderson, C. W. M. Kay, A. Bagno, F. Rastrelli, Y. Murata, K. Komatsu, X. Lei, Y. Li, N. J. Turro, M. H. Levitt and J. J. L. Morton, *Philosophical Transactions of the Royal Society A: Mathematical, Physical and Engineering Sciences*, 2013, **371**, 20120475.

20 S. Mamone, M. Ge, D. Hüvonen, U. Nagel, A. Danquigny, F. Cuda, M. C. Grossel, Y. Murata, K. Komatsu, M. H. Levitt, T. Rõõm and M. Carravetta, *The Journal of Chemical Physics*, 2009, **130**, 081103.

21 M. Ge, U. Nagel, D. Hüvonen, T. Rõõm, S. Mamone, M. H. Levitt, M. Carravetta, Y. Murata, K. Komatsu, J. Y.-C. Chen and N. J. Turro, *The Journal of Chemical Physics*, 2011, **134**, 054507.

22 T. Rõõm, L. Peedu, M. Ge, D. Hüvonen, U. Nagel, S. Ye, M. Xu, Z. Bačić, S. Mamone, M. H. Levitt, M. Carravetta, J. Y.-C. Chen, X. Lei, N. J. Turro, Y. Murata and K. Komatsu, *Philosophical Transactions of the Royal Society A: Mathematical, Physical and Engineering Sciences*, 2013, **371**, 20110631.

23 A. J. Horsewill, S. Rols, M. R. Johnson, Y. Murata, M. Murata, K. Komatsu, M. Carravetta, S. Mamone, M. H. Levitt, J. Y. C. Chen, J. A. Johnson, X. Lei and N. J. Turro, *Physical Review B*, 2010, **82**, 081410.

24 A. J. Horsewill, K. S. Panesar, S. Rols, J. Ollivier, M. R. Johnson, M. Carravetta, S. Mamone, M. H. Levitt, Y. Murata, K. Komatsu, J. Y.-C. Chen, J. A. Johnson, X. Lei and N. J. Turro, *Physical Review B*, 2012, **85**, 205440.

25 A. J. Horsewill, K. Goh, S. Rols, J. Ollivier, M. R. Johnson, M. H. Levitt, M. Carravetta, S. Mamone, Y. Murata, J. Y.-C. Chen, J. A. Johnson, X. Lei and N. J. Turro, *Philosophical Transactions of the Royal Society A: Mathematical, Physical and Engineering Sciences*, 2013, **371**, 20110627.

26 M. Xu, M. Jiménez-Ruiz, M. R. Johnson, S. Rols, S. Ye, M. Carravetta, M. S. Denning, X. Lei, Z. Bačić and A. J. Horsewill, *Physical Review Letters*, 2014, **113**, 123001.

27 S. Mamone, J. Y.-C. Chen, R. Bhattacharyya, M. H. Levitt, R. G. Lawler, A. J. Horsewill, T. Rõõm, Z. Bačić and N. J. Turro, *Coordination Chemistry Reviews*, 2011, **255**, 938–948.

28 K. S. K. Goh, M. Jiménez-Ruiz, M. R. Johnson, S. Rols, J. Ollivier, M. S. Denning, S. Mamone, M. H. Levitt, X. Lei, Y. Li, N. J. Turro, Y. Murata and A. J. Horsewill, *Physical Chemistry Chemical Physics*, 2014, **16**, 21330–21339.

29 Y. Li, X. Lei, S. Jockusch, J. Y.-C. Chen, M. Frunzi, J. A. Johnson, R. G. Lawler, Y. Murata, M. Murata, K. Komatsu and N. J. Turro, *Journal of the American Chemical Society*, 2010, **132**, 4042–4043.

30 Y. Li, X. Lei, R. G. Lawler, Y. Murata, K. Komatsu and N. J. Turro, *The Journal of Physical Chemistry Letters*, 2011, **2**, 741–744.

31 Y. Kohama, T. Rachi, J. Jing, Z. Li, J. Tang, R. Kumashiro, S. Izumisawa, H. Kawaji, T. Atake, H. Sawa, Y. Murata, K. Komatsu and K. Tanigaki, *Physical Review Letters*, 2009, **103**, 073001.

32 M. S. Dresselhaus, G. Dresselhaus and P. C. Eklund, *Science of Fullerenes and Carbon Nanotubes*, Academic Press, 1996.

33 R. Tycko, G. Dabbagh, R. M. Fleming, R. C. Haddon, A. V. Makhija and S. M. Zahurak, *Physical Review Letters*, 1991, **67**, 1886–1889.

34 P. A. Heiney, *Journal of Physics and Chemistry of Solids*, 1992, **53**, 1333–1352.

35 W. I. F. David, R. M. Ibberson, T. J. S. Dennis, J. P. Hare and K. Prassides, *Europhysics Letters (EPL)*, 1992, **18**, 219–225.

36 W. I. F. David, R. M. Ibberson, T. J. S. Dennis, J. P. Hare and K. Prassides, *Europhysics Letters (EPL)*, 1992, **18**, 735–736.

37 B. Sundqvist, *Advances in Physics*, 1999, **48**, 1–134.

38 A. J. Horsewill, K. S. Panesar, S. Rols, M. R. Johnson, Y. Mu-

rata, K. Komatsu, S. Mamone, A. Danquigny, F. Cuda, S. Maltsev, M. C. Grossel, M. Carravetta and M. H. Levitt, *Physical Review Letters*, 2009, **102**, 013001.

39 *The yellow book*, 2008, http://www.ill.eu/instruments-support/instruments-groups/yellowbook.

40 A. J. Horsewill, K. Goh, M. R. Johnson, M. H. Levitt, S. Mamone, J. Ollivier, S. Rols and N. J. Turro, *Quantum dynamics of H2 in the endofullerene H2@C60: Crystal field effects and fine structure in the J=0 to J=1 rotational line*, 2014, http://doi.ill.fr/10.5291/ILL-DATA.7-05-412.

41 D. A. Varshalovich, A. N. Moskalev and V. K. Khersonskii, *Quantum Theory of Angular Momentum*, World Scientific, Singapore, 1988.

42 F. Reif and E. M. Purcell, *Physical Review*, 1953, **91**, 631–641.

43 T. Yildirim and A. B. Harris, *Physical Review B*, 2002, **66**, 214301.

44 M. Abramowitz and I. A. Stegun, *Handbook of Mathematical Functions: with Formulas, Graphs, and Mathematical Tables*, Dover Publications, Ninth Dover Printing edn, 1972.